Negative ion photoelectron spectroscopy of the AsO^- anion

T. P. Lippa, S.-J. Xu, S. A. Lyapustina, and K. H. Bowen[a)]
Department of Chemistry, Johns Hopkins University, Baltimore, Maryland 21218

(Received 17 August 1998; accepted 28 August 1998)

The negative ion photoelectron spectrum of AsO^- has been measured, assigned, and analyzed. The adiabatic electron affinity, EA_a, was determined directly from the photoelectron spectrum. The dissociation energy of AsO^-, $D_0(AsO^-)$, was computed via an energetic cycle using our measured value of EA_a and existing literature values for other necessary quantities. Franck–Condon analysis provided values for the bond length of the AsO^- anion, $r_e(AsO^-)$, its vibrational frequency, $\omega_e(AsO^-)$, and its anharmonicity constant, $\omega_e\chi_e(AsO^-)$. The values of the molecular constants which were determined in this work are: $EA_a(AsO)=1.286\pm0.008$ eV, $D_0(AsO^-)=4.74\pm0.08$ eV, $r_e(AsO^-)=1.696\pm0.010$ Å, $\omega_e(AsO^-)=827\pm40$ cm^{-1}, and $\omega_e\chi_e(AsO^-)=5.54$ cm^{-1}. In addition, we determined the $X\ ^3\Sigma^- - a\ ^1\Delta$, ground-to-first excited state splitting in AsO^- to be $\sim$0.54 eV. © *1998 American Institute of Physics.* [S0021-9606(98)01945-X]

I. INTRODUCTION

The molecular constants of the diatomic radical, AsO, have been determined by Fourier transform infrared (FTIR) absorption spectroscopy,[1] infrared diode laser spectroscopy,[2] electronic emission spectroscopy,[3–6] chemiluminescence studies,[7] and mass spectrometric equilibrium measurements.[8] The electronic spectra of AsO and related diatomic molecules have also been the subject of a review article.[9] In addition, theoretical studies[10–12] on the low-lying states of AsO have provided potential energy curves, dipole moments, and transition probabilities. While the neutral molecule is relatively well studied, apparently no work has been reported on the molecular anion, AsO^-, the closest pertinent investigations being negative ion photoelectron spectroscopic studies[13,14] of the isoelectronic species, NO^- and PO^-. Here, we report the negative ion photoelectron (photodetachment) spectrum of AsO^-.

II. EXPERIMENT

Negative ion photoelectron spectroscopy is conducted by crossing a mass-selected negative ion beam with a fixed-frequency photon beam and energy-analyzing the resultant photodetached electrons. The mass selector used in these experiments was a Wein (E×B) filter. The photon source was an argon ion laser operated intracavity. The electron energy analyzer was a single channel, hemispherical instrument. Our apparatus has been described in detail previously.[15]

The negative ion photoelectron spectroscopic technique is a direct approach for determining electron binding energies (EBE), relying on the relationship,

$$h\nu = \mathrm{EBE} + \mathrm{KE}_e . \tag{1}$$

in which $h\nu$ is the photon energy, and KE_e is the measured photoelectron kinetic energy. The photoelectron spectrum of AsO^- was calibrated against the well-known photoelectron spectra[13,16] of O^- and of NO^- and was recorded with a photon energy of 2.497 eV.

Arsenic oxide anions were generated in a hot, supersonic expansion ion source by heating elemental arsenic to 650–700 K in the argon-filled ($\sim$3 atm.) stagnation chamber of the source. The resulting arsenic vapor was coexpanded with argon through a 125 μm nozzle orifice. This expansion was intercepted just outside the nozzle orifice by an effusive flow of N_2O from a nearby ''pickup'' line. In this same region, anions were formed by injection of electrons from a thoriated-iridium filament directly into the expanding jet in the presence of an axial magnetic field. Typically, the filament was biased at -75 V relative to the stagnation chamber, giving an emission current of $\sim$10 mA. The stagnation chamber itself was floated at -500 V, i.e., the beam energy. Under these conditions, this ion source provided $\sim$50 pA of AsO^- ion current at the ion/photon interaction region of the spectrometer.

III. RESULTS AND DISCUSSION

The photoelectron (photodetachment) spectrum of AsO^-, recorded with 2.497 eV photons, is presented in Fig. 1. In photodetachment ''transitions'', the initial state is that of the anion, while the final states are those of its corresponding neutral. In analogy[14] with PO^-, the low-lying electronic states of AsO^-, are $^3\Sigma^-$, $^1\Delta$, and $^1\Sigma^+$, where the energy ordering is $X\ ^3\Sigma^-$, $a\ ^1\Delta$, and $b\ ^1\Sigma^+$. The ground state of neutral AsO is $^2\Pi_r$, with a 1026 cm^{-1} spin-orbit splitting.[17] Since the vibrational frequency, ω_e, for the ground state is 967 cm^{-1}, there is a near coincidence of vibrational levels from the two spin-orbit components, beginning at $v=1$ in $^2\Pi_{1/2}$ and $v=0$ in $^2\Pi_{3/2}$. The first excited state of neutral AsO is over 3 eV higher in energy and is beyond the photon energy used in this work. Thus, we attribute the observed vibronic profile in Fig. 1 primarily to AsO $(^2\Pi_{3/2,1/2}, v') \leftarrow AsO^-(X\ ^3\Sigma^-, v'')$ transitions.

[a)]Author to whom correspondence should be addressed.

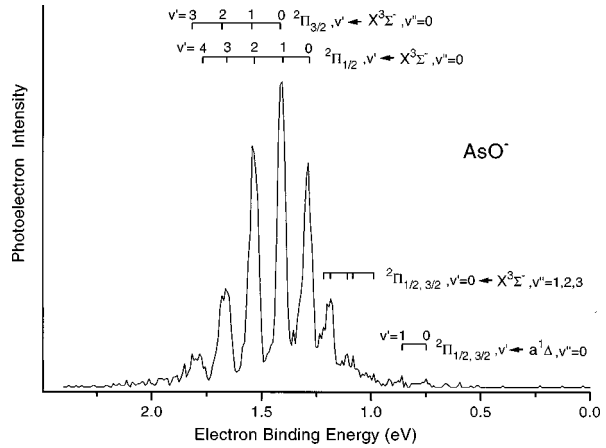

FIG. 1. The assigned photoelectron spectrum of AsO^- recorded with 2.497 eV photons.

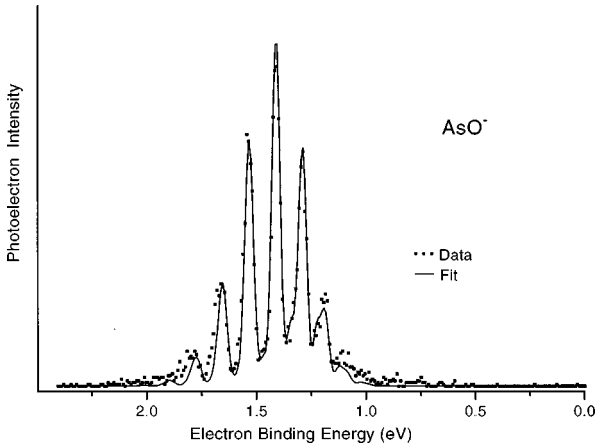

FIG. 2. A comparison of the experimental and the modeled photoelectron spectrum of AsO^-.

The vibrational spacings observed toward the high EBE side of this spectral profile compare reasonably well with the 119.9 meV literature value[17] for the vibrational frequency of neutral AsO, while the vibrational spacings at the low EBE side of the profile are somewhat smaller. Given that the vibrational frequency of AsO^- is expected to be smaller than that of AsO (based on bonding arguments and analogy with PO^-), and the fact that hot bands appear most prominently on the low EBE side of vibronic profiles, the assignment of the spectrum was straightforward in most regions and is indicated in Fig. 1. The origin transition, i.e., the $AsO(^2\Pi_{1/2}, v'=0) \leftarrow AsO^-(X\ ^3\Sigma^-, v''=0)$ transition, was assigned based on the observations that the spacing between it and the next highest EBE peak is 119.6 meV, while the spacing between it and the next lowest EBE peak is 102.6 meV. The EBE of this transition is equal to the value of the adiabatic electron affinity, EA_a, and for AsO, we have thus determined EA_a to be 1.286 ± 0.008 eV.

The peaks immediately to the low EBE side of the origin peak are assigned and labeled as vibrational hot bands arising from the $v''=1,2,3...$ levels of the $X\ ^3\Sigma^-$ state of AsO^-. The two weaker features at even lower EBE do not follow the vibrational hot band progression in energy spacing. These are probably electronic hot bands from the $a\ ^1\Delta$ excited state of AsO^-. Since the spacing between these features is comparable with the vibrational spacing in the ground state of AsO, we assign the lower EBE feature (as indicated in Fig. 1) to be the $AsO(^2\Pi_{1/2}, v'=0) \leftarrow AsO^-(a\ ^1\Delta, v''=0)$ transition. The difference between the EBE of this transition and EA_a is $T_0(X\ ^3\Sigma^- - a\ ^1\Delta)$, which we find to be ~ 0.54 eV. (The $X\ ^3\Sigma^- - a\ ^1\Delta$ splitting in PO^- is ~ 0.55 eV.)[14]

The relationship between $EA_a(AsO)$, $EA(O)$, $D_0(AsO)$, and $D_0(AsO^-)$, where $D_0(AsO^-)$ pertains to AsO^- dissociating into the atomic ground states of As and O^- is

$$EA_a(AsO) - EA(O) = D_0(AsO^-) - D_0(AsO). \quad (2)$$

Having determined $EA_a(AsO)$ and knowing the literature values[8,16] of EA(O) to be 1.465 eV and $D_0(AsO)$ to be 4.92 eV, we computed the value of $D_0(AsO^-)$ to be 4.74 ± 0.08 eV. This is consistent with the expectation that AsO^- would have a weaker bond than AsO.

Franck–Condon analysis of the AsO^- photoelectron spectrum corroborated our assignment of the spectrum and provided values for several molecular constants. This analysis was conducted using a program developed by Ervin and Lineberger.[18] It models both anion and neutral electronic potential curves as Morse oscillators. The final fitted spectrum was the result of modeling transitions to two separate neutral potential energy curves (one for each of the spin-orbit components) and combining their intensities. The additive effect of these two transitions is the reason that the peak labeled as both $^2\Pi_{1/2},\ v'=1 \leftarrow X\ ^3\Sigma^-,\ v''=0$ and $^2\Pi_{3/2},\ v'=0 \leftarrow X\ ^3\Sigma^-,\ v''=0$ in Fig. 1, is the strongest intensity peak in the spectrum. The input parameters for neutral AsO [$r_e(AsO) = 1.6236\ A$, $\omega_e(AsO) = 967.08\ cm_{-1}$, and $\omega_e\chi_e(AsO) = 4.85\ cm^{-1}$] were taken from the literature. Optimization of the fit gave the following molecular constants for the AsO^- anion: $r_e(AsO^-) = 1.696 \pm 0.010\ A$, $\omega_e(AsO^-) = 827 \pm 40\ cm^{-1}$, $\omega_e\chi_e(AsO^-) = 5.54\ cm^{-1}$ (see Fig. 2 and Table I). These values are intuitively consistent with expec-

TABLE I. Periodic trends in molecular constants for the Group VB(15) diatomic oxides and their anions.

Molecule	EA_a (eV)	r_e (Å)	ω_e (cm^{-1})	D_0 (eV)
NO	0.026[a]	1.151	1904	6.50
PO	1.092[b]	1.476	1233	6.15
AsO	1.286[c]	1.624	967	4.92[e]
SbO	···	1.825	816	<4.39
BiO	···	1.934	692	3.47
NO^-		1.271[a]	1284[d]	5.06
PO^-		1.54[b]	1000[b]	5.78[b]
AsO^-		1.69[c]	827[c]	4.74[c]

[a]Reference 13.
[b]Ref. 14; ω_e was not explicitly reported. This value is actually $\nu_{01}(X\ ^3\Sigma^- PO^-)$.
[c]This work.
[d]Reference 19.
[e]Reference 8.

tations. AsO^- is expected to have a weaker bond than AsO and thus, a longer bond length and a smaller vibrational frequency. The optimized fit also gave a temperature of 1050 K. While this temperature is higher than one might have expected, it may reflect the fact that the anion temperature is governed not only by the source temperature, but also by the exothermicity of the chemical reaction which formed it in the pickup region.

It is interesting to compare, insofar as data is available, the periodic trends in molecular constants among the Group VB (15) diatomic oxides and their anions. Table I tabulates some of these values. Adiabatic electron affinities increase as one descends the periodic column, with a particularly steep increase seen in going from $EA_a(NO)$ to $EA_a(PO)$. While there appear to be no values available for the electron affinities of SbO and BiO, it can be anticipated that $EA_a(SbO)$ is larger than 1.286 eV, and that $EA_a(BiO)$ is greater than $EA_a(SbO)$. The addition of an electron to each of the neutrals to form their anions causes the bond lengths of the anions to increase relative to the bond lengths of their corresponding neutrals. Again, there is essentially no information available about the molecular constants of SbO^- and BiO^-. Presumably, however, $r_e(SbO^-)$ is greater than 1.825 Å, and $r_e(BiO^-)$ is greater than 1.934 Å. Weaker bonds in the anions as compared to their corresponding neutrals also leads to smaller values for vibrational frequencies in the anions relative to their neutrals. We anticipate that $\omega_e(SbO^-)$ is smaller than 816 cm^{-1}, and that $\omega_e(BiO^-)$ is smaller than 692 cm^{-1}. Since the anions have weaker bonds than their corresponding neutrals, it follows that the dissociation energies of the anions should be smaller than those of their neutrals, and this is what is seen. Upon descending the periodic column, however, one notices that the values of the tabulated anion dissociation energies do not decrease monotonically. This is because $D_0(NO^-)$ is anomalously small, which in turn is related to $EA_a(NO)$ being so much smaller than the adiabatic electron affinities of the other Group VB diatomic oxides. Inequalities, analogous to those discussed above, are also expected for $D_0(SbO^-)$ and $D_0(BiO^-)$.

ACKNOWLEDGMENTS

This work was supported by the Division of Materials Science, Office of Basic Energy Sciences, U.S. Department of Energy under Grant No. DE-FG02-95ER45538. Acknowledgment is also made to The Donors of the Petroleum Research Fund, administered by the American Chemical Society, for partial support of this research (Grant No. 28452-AC6).

[1] F. Ito, T. Nakanaga, H. Takeo, K. Essig, and H. Jones, J. Mol. Spectrosc. **174**, 417 (1995).
[2] K. Essig, H. Jones, F. Ito, and H. Takeo, J. Mol. Spectrosc. **170**, 152 (1995).
[3] J. H. Callomon and J. E. Morgan, Proc. Phys. Soc. London **86**, 1091 (1965).
[4] S. Mrozovski and C. Santaram, J. Opt. Soc. Am. **56**, 1174 (1966).
[5] V. M. Anderson and J. H. Callomon, J. Phys. B **6**, 1664 (1973).
[6] R. R. Reddy and T. V. R. Rao, J. Quant. Spectrosc. Radiat. Transf. **33**, 415 (1985).
[7] V. S. Kushawaha, Chem. Phys. Lett. **30**, 130 (1975).
[8] K. H. Lau, R. D. Brittain, and D. L. Hildenbrand, Chem. Phys. Lett. **81**, 227 (1981).
[9] S. B. Rai and D. K. Rai, Chem. Rev. **84**, 73 (1984).
[10] A. B. Alekseyev, A. B. Sannigrahi, H.-P. Liebermann, R. J. Buenker, and G. Hirsch, J. Chem. Phys. **103**, 234 (1995).
[11] M. L. P. Rao, T. Savithry, D. V. K. Rao, and P. T. Rao, Indian J. Pure Appl. Phys. **14**, 504 (1976).
[12] S. V. J. Lakshman and T. V. Ramakrishna Rao, J. Phys. B **4**, 269 (1971).
[13] M. J. Travers, D. C. Cowles, and G. B. Ellison, Chem. Phys. Lett. **164**, 449 (1989).
[14] P. F. Zittel and W. C. Lineberger, J. Chem. Phys. **65**, 1236 (1976).
[15] J. V. Coe, J. T. Snodgrass, C. B. Freidhoff, K. M. McHugh, and K. H. Bowen, J. Chem. Phys. **84**, 618 (1986).
[16] P. M. Dehmer and W. A. Chupka, J. Chem. Phys. **62**, 4525 (1975).
[17] K. P. Huber and G. Herzberg, *Molecular Spectra and Molecular Structure* (Van Nostrand Reinhold, New York, 1979), Vol. 4.
[18] PESCAL Fortran program, written by K. M. Ervin and W. C. Lineberger.
[19] C. Amoit, R. Bacis, and G. Guelachvilli, Can. J. Phys. **56**, 251 (1978).